

N87-11191

## TURBINE AIRFOIL DEPOSITION MODELS

Daniel E. Rosner  
Yale University  
Department of Chemical Engineering  
High Temperature Chemical Reaction Engineering Laboratory

## 1. INTRODUCTION, OUTLINE

Gas turbine failures associated with sea-salt ingestion and sulfur-containing fuel impurities have directed attention to alkali sulfate deposition and the associated "hot corrosion" of gas turbine (GT) blades under some GT operating conditions. These salts deposit and form thin, molten films which undermine the protective metal oxide coating normally found on GT blades. This research project deals with the prediction of molten salt deposition, flow and oxide dissolution and their effects on the lifetime of turbine blades. Our goals include rationalizing and helping to predict corrosion patterns on operational GT rotor blades and stators, and ultimately providing some of the tools required to design laboratory simulators and future corrosion-resistant high-performance engines. In the program summary below, we first review necessary background developments\* (Sections 2, 3 and 4) and then introduce our recent results and tentative conclusions (Sections 5, 6), along with a brief account of our present research plans.

## 2. VAPOR DEPOSITION (VD-) RATE THEORY

The first step in a complex sequence of events leading to hot corrosion failures is the deposition of alkali salts from the combustion products onto turbine stator vanes and rotor blades. Our NASA-supported laboratory experiments,<sup>1-3</sup> and those carried out in collaboration with NASA-Lewis Research Laboratories,<sup>4</sup> have enabled advances in salt deposition rate theory, as briefly outlined here. A comprehensive but tractable method for predicting the rates of chemical vapor deposition (CVD) of, say, alkali sulfates from multicomponent salt-laden combustion products was first developed, illustrated and tested in part.<sup>4,5,8</sup> This theory predicts important effects of multicomponent diffusion and thermal (Soret) diffusion<sup>6</sup> on dew points, CVD-rates and deposit compositions.<sup>7</sup> For present purposes an important feature of the deposition rate is its dependence on surface temperature, which ordinarily reveals the existence of a dew point temperature (above which a macroscopic surface condensate is not stable) and a temperature-insensitive plateau deposition rate at temperatures sufficiently far below the dew point — i.e., features included in the above-mentioned CVD-rate theory.<sup>4,5,7,8</sup> While in its most general form, allowance is made for the transport of each chemical species ( $i = 1, 2, \dots$ ) containing the elements of interest (Na, S ...) across the diffusion boundary layer (BL) (Fig. 1), to study the dynamics of the resulting molten salt condensate layer (Section 3 below), we use the single-component limiting form of the CVD theory to economically provide the spatial distribution of condensate "arrival." This approach also applies without fundamental modifications to the deposition rate of pre-existing fine particles,<sup>9,10</sup> i.e., mist droplets small enough to behave like "heavy molecules" in the prevailing carrier gas flow field. The inclusion of chemical reactions and/or phase change (e.g., "mist formation") within the BL requires further research, some of which is in progress (Section 6).

\*and update bibliographic information on our recently published papers.

† NAG 3-201

### 3. CONDENSATE LAYER DYNAMICS

An important process in the molten salt attack of GT blades is evidently the dissolution ("fluxing") of the normally protective metal oxide, and this in turn, implies dynamic processes which allow dissolution/reaction to occur without saturating the molten salt solvent. For these reasons, we have carried out studies of the dynamics of thin condensate liquid layers<sup>11</sup>, allowing for the interplay of salt arrival rate (Section 2) and runoff induced by aerodynamic shear stress  $\tau_w$  and blade rotation rate,  $\Omega$  (Fig. 2). These studies should ultimately prove useful in the interpretation of observed hot corrosion maps on blades removed from operational engines. They have already guided the development and interpretation of laboratory simulator experiments<sup>3,4,8</sup> in which molten salt deposition and runoff necessarily occur at seed levels such that  $T_{dp} > T_{mp}$ .

In ref. 11 the necessary liquid layer theory was developed and used to predict steady-state laminar single component condensate layers on smooth non-rotating, isothermal targets, with emphasis on the circular cylinder in high Reynolds number cross-flow (a common test configuration). In our recent studies, this approach has been extended to include the treatment of single component condensate layer flow along smooth non-isothermal rotor blades (Fig. 2). Illustrative calculations have thus far been made for a test turbine (NASA TP 1018 (1977)), but most of our methods will carry over to operational engine vanes and blades (except in the immediate vicinity of cooling slots/holes). From the inviscid stream velocity data, we compute, using efficient integral methods, the corresponding distributions of gas-side momentum; heat- and mass-transfer coefficients, and the distribution of blade "recovery" temperature (used to estimate this root-cooled blade temperature distribution). The corresponding condensate arrival rate distribution and liquid viscosity distributions are then inserted into the partial differential equation (PDE) governing the liquid layer thickness  $\delta_\ell(x,z)$  (Fig. 2). This nonlinear first-order PDE is numerically solved (by the method-of-characteristics) to provide the condensate layer streamline pattern (Fig. 3), as well as the corresponding liquid layer thickness  $\delta_\ell(x,z)$ . Two important by-products of these calculations are (a) the solvent inventory on the blade, and (b) relative tip and trailing edge salt runoff rates. It is also interesting to note that surface flow can lead to the presence of condensate on portions of the blade which are hotter than the prevailing dew point. One such region is shown in Fig. 4, in which the span-wise flow associated with blade rotation causes the steady-state presence of molten salt at  $T_w > T_{dp}$ , and hence, the possibility of appreciable local hot corrosion rates above  $T_{dp}$ .

### 4. METAL OXIDE "DISSOLUTION" RATE DISTRIBUTIONS

As mentioned at the outset of Section 3, non-stoichiometric molten sodium sulfate is known to be a solvent for  $Al_2O_3(s)$  or  $Cr_2O_3(s)$  — the oxides ordinarily relied upon for corrosion protection of the underlying blade alloys. Accordingly, we have utilized the above-mentioned formulation to predict dissolution rate distributions associated with solvent flow patterns of the type shown (Fig. 3). Indeed, it will be instructive to compare such predictions with hot corrosion rate patterns observed on blades removed from operational GT engines. Toward this end, estimates have been made of the oxide diffusion coefficient in the solvent, equilibrium solubility, and maximum (kinetic) rate of dissolution. This information was then used to predict the solute diffusion-limited dissolution rate along each streamline (cf. Fig. 5) using a generalization of Leveque-Levich BL-theory. The corresponding arrival rate distribution is shown in Fig. 6 for comparison. Preliminary dissolution rate maps are being checked, generalized and discussed in terms of their parametric dependencies, and to the limited extent possible, agreement with operational experience. This research will be summarized in our final report on Grant NAG 3-201, and in a paper<sup>12</sup> currently in preparation. Publication seems to be timely, since even though high-quality operational data are not generally available, we believe that the formalism we have developed will make possible in the U.S.-GT industry instructive and economical parametric studies for both stator and rotor

blades over a wide variety of environmental conditions (salt level, turbine inlet temperature, stagnation pressure level, blade contour and cooling, tip speed, etc.). Moreover, the stage has been set to generalize many aspects of the theory, including commonly encountered mixed alkali deposits, condensate arrival by both vapor diffusion and thermophoretic capture of BL-nucleated droplets,<sup>13</sup> and transient condensate flows. It should also be useful to examine in greater detail the effects on localized dissolution rates of secondary flows, produced in part by surface tension gradients associated with the oxide dissolution process itself.

## 5. PRELIMINARY INVESTIGATION OF BINARY CONDENSATE LAYER EFFECTS

All properties of thin liquid condensate films, including their aggressiveness as corro-dants, are expected to be composition-dependent. Moreover, appreciable amounts of adulter-ants (e.g. Ca- and Mg-compounds) are often found in GT-blade deposits upon engine shut-down and blade removal. This information, combined with the remarkable effect the addition of a second salt can have on the deposition rate of the primary salt (see ref. 14, based on our experiments carried out under NASA Grant NSG 3169) suggests that attention should be directed toward the deposition, dynamics and dissolution rate properties of multicomponent molten salt layers, not just the behavior of pure  $\text{Na}_2\text{SO}_4$ ( $l$ ). Toward this end, we are proposing intensive studies of the expected behavior of binary sulfate salt layers.

Among the effects anticipated for binary molten salt cases, perhaps the most significant are the alteration of:

- (a) deposition rates and associated dew point temperature,
- (b) liquid properties, including the important oxide solubility and associated Fick diffusivity,
- (c) freezing point of the solution.

While the property effects (b) remain to be studied, it is clear that effects (a) and (c) can considerably broaden the important temperature interval:  $T_{dp} - T_{mp}$  within which hot corro-sion is known to take its toll on GT blade alloys.

To illustrate the consequences of the altered freezing point, we have performed a prelim-inary steady-state analysis of the binary ( $\text{K}_2\text{SO}_4 + \text{Na}_2\text{SO}_4$ ) condensate layer expected along the leading edge of a non-isothermal (root-cooled) rotor blade, with a specified root temperature (cf.  $T_{mp}(\text{Na}_2\text{SO}_4) = 1157\text{K}$  and  $T_{mp}(\text{K}_2\text{SO}_4) = 1343\text{K}$ ) and  $\Omega = 6786$  rad/s. Figure 7 reveals that if  $T_v(0,0)$  is as low as 1110K then the condensate on the leading edge would be entirely solid in the absence of potassium addition to the mainstream (with  $T_{dp}(\text{Na}_2\text{SO}_4) = 1242\text{K}$ ). However, with increasing potassium levels, an increasing fraction of the condensate would become molten (becoming fully molten at  $([\text{K}]/[\text{Na}])_\infty$ -ratios above about 0.13. More comprehensive prototyp-ical examples, including effects (a), (b) and (c) above, are planned.

## 6. TENTATIVE CONCLUSIONS, IMPLICATIONS, FUTURE WORK

While much of the required input information remains to be sharpened up (based on inde-pendent experiments), we believe that the present formalism has reached the point where instructive parametric studies can now be economically performed for both GT stator vanes and rotor blades over a wide variety of environmental conditions (salt level, turbine inlet temperature, stagnation pressure level, blade contour and cooling, tip speed, etc.).

For the present, the following conclusions have emerged from our recent investigations:

- (a) On rotor blades, qualitatively different condensate behavior (thickness, composition) is observed depending upon whether the liquid streamlines emerge from the blade lead-ing edge or root (see e.g. Fig. 3).

- (b) For surfaces everywhere below  $T_{dp}$  predicted oxide dissolution rate distributions (Fig. 5) are strongly coupled to the predicted local condensate arrival rate distribution (Fig. 6).

This observation, combined with formal computations which presume highly undersaturated liquid layers, lead us to conclude that:

- (c) The tendency toward local saturation of the condensate layer strongly influences the distribution of metal oxide dissolution rate.
- (d) Owing to liquid layer convection across blade isotherms, liquid layers (hence corrosion) can occur on some areas of a GT blade which are above the prevailing dew point temperature.
- (e) The simultaneous presence of chemical elements capable of entering into the condensate solution considerably broadens the temperature interval  $T_{dp}-T_{mp}$  (within which hot corrosion is likely to take its toll on GT blade alloys) but improves the chances of reduced deposition rates via BL mist formation.<sup>13,14</sup>

Finally, we realize that to fully exploit and test the presently developed liquid layer theory:

- (f) Additional fundamental data will be needed (e.g. temperature and stoichiometry dependence of the solubility of  $Al_2O_3$  and  $Cr_2O_3$  in  $Na_2SO_4(l)$ ).
- (g) Well-documented test data on hot-corrosion rate distributions from simulated and/or real turbine blades run under nearly constant environmental conditions will be needed.

## 7. REFERENCES

1. Rosner, D. E. and Atkins, R. M., in Fouling and Slagging Resulting from Impurities in Combustion Gases (R. Bryers, ed.) Engineering Foundation (New York) 1983, pp. 469-492.
2. Rosner, D. E. and Seshadri, K., in Eighteenth Int. Symposium on Combustion, The Combustion Institute (Pittsburgh, PA), 1981, pp. 1385-1394.
3. Seshadri, K. and Rosner, D. E., AIChE J. **30**(2), 187 (1984).
4. Kohl, F. J., Santoro, G. J., Stearns, C. A., Fryburg, G. C. and Rosner, D. E., J. Electrochem. Soc. **126**, 1054 (1979).
5. Rosner, D. E., Chen, B.-K., Fryburg, G. C. and Kohl, F. J., Comb. Sci. and Tech. **20**, 87 (1979).
6. Rosner, D. E., J. Physicochem. Hydrodynamics **1**, 159 (1980).
7. Rosner, D. E. and Nagarajan, R., "Transport-Induced Shifts in Condensate Dew Point and Composition in Multicomponent Systems with Chemical Reaction," Chemical Engrg. Sci. (in press, 1984).

8. Santoro, G. J., Kohl, F. J., Stearns, C. A., Rosner, D. E. and Gokoglu, S. A., Experimental and Theoretical Deposition Rates from Salt-seeded Combustion Gases of a Mach 0.3 Burner Rig, NASA TP 225 (1984).
9. Gokoglu, S. A. and Rosner, D. E., Int. J. Heat and Mass Trans. 27, 639 (1984).
10. Rosner, D. E., Gokoglu, S. A. and Israel, R., in Fouling of Heat Exchange Surfaces (R. Bryers, ed.) Engineering Foundation (New York) 1983, pp. 235-256.
11. Rosner, D. E., Gunes, D. and Anous, N., Chem. Engrg. Commun. 24, 275 (1983).
12. Rosner, D. E. and Nagarajan, R., "Theoretical Model to Predict/Understand the Corrosion Rate Consequences of Molten Alkali Sulfate Condensation on Combustion Turbine Blades" (in preparation, 1984).
13. Castillo, J. L. and Rosner, D. E., "Mass Transfer Consequences of Droplet Thermophoresis and Local Vapor/Liquid Equilibrium in Dilute Binary Condensible Vapor Laminar Boundary Layers" (in preparation, 1984).
14. Rosner, D. E. and Liang, B., "Development and Demonstration of Flash Evaporation Technique for Binary Alkali Sulfate Salt-Seeded Flames" (in preparation, 1984).

VAPOR DEPOSITION  
Multi-component  
"CFBL" Theory

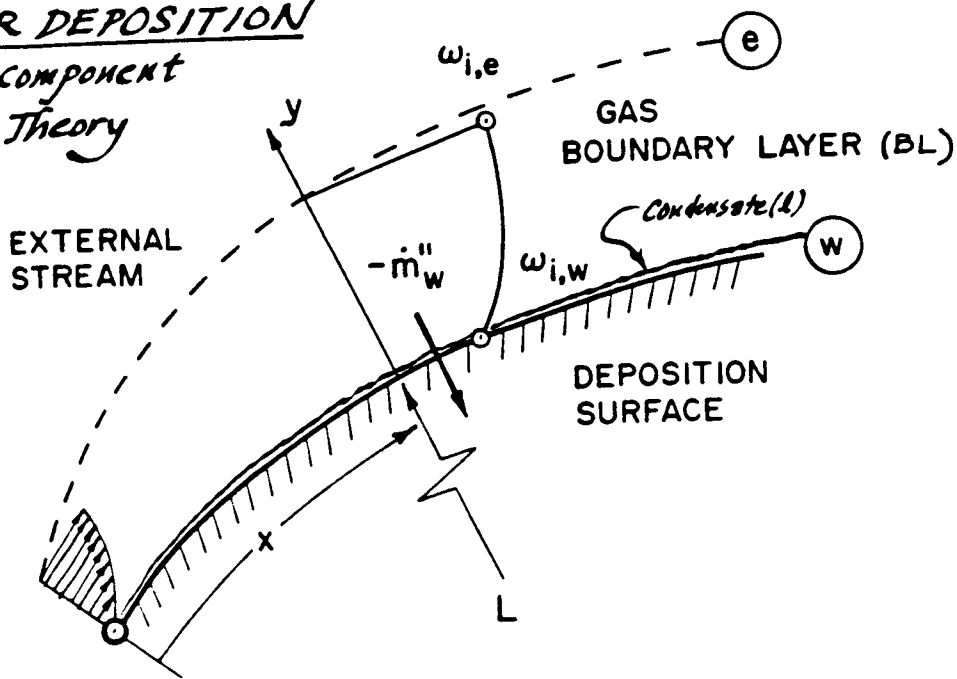
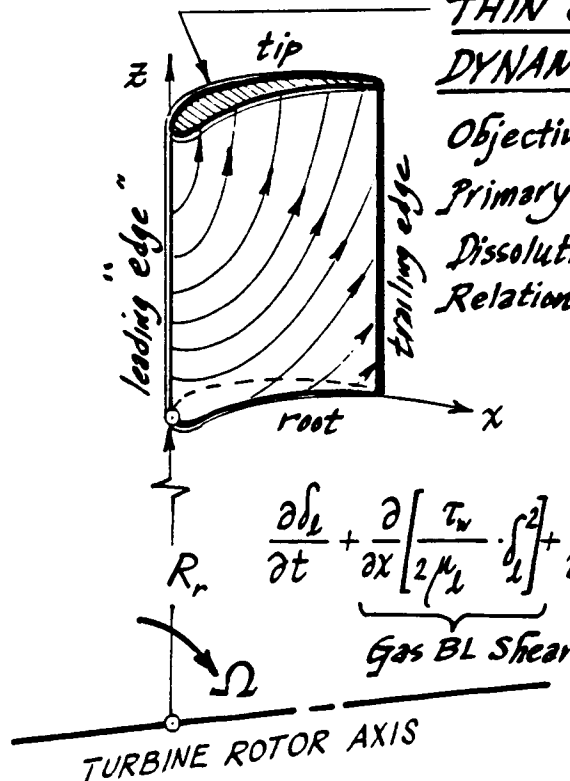


Fig. 1: Vapor phase boundary layer near turbine blade surface source of momentum and mass for thin condensate layer.

THIN CONDENSATE LAYER  
DYNAMICS - ROTOR BLADES

Objectives:  
Primary Flow, and its Metal Oxide  
Dissolution Rate Consequences;  
Relation to observed hot corrosion patterns?



"Centrifugal" term      "Arrival" from Vapor BL

$$\frac{\partial \delta_L}{\partial t} + \underbrace{\frac{\partial}{\partial x} \left[ \frac{\tau_w}{2\mu_L} \cdot \int_0^{\delta_L} dz \right]}_{\text{Gas BL Shear}} + \frac{\partial}{\partial z} \left[ \frac{\Omega^2 (R_r + z)}{3\nu_L} \cdot \int_0^{\delta_L} z^3 dz \right] = \frac{-\dot{m}''(x, z, t)}{\rho_L}$$

Fig. 2: Factors influencing the evolution of liquid condensate layer dynamics on a turbine rotor blade.

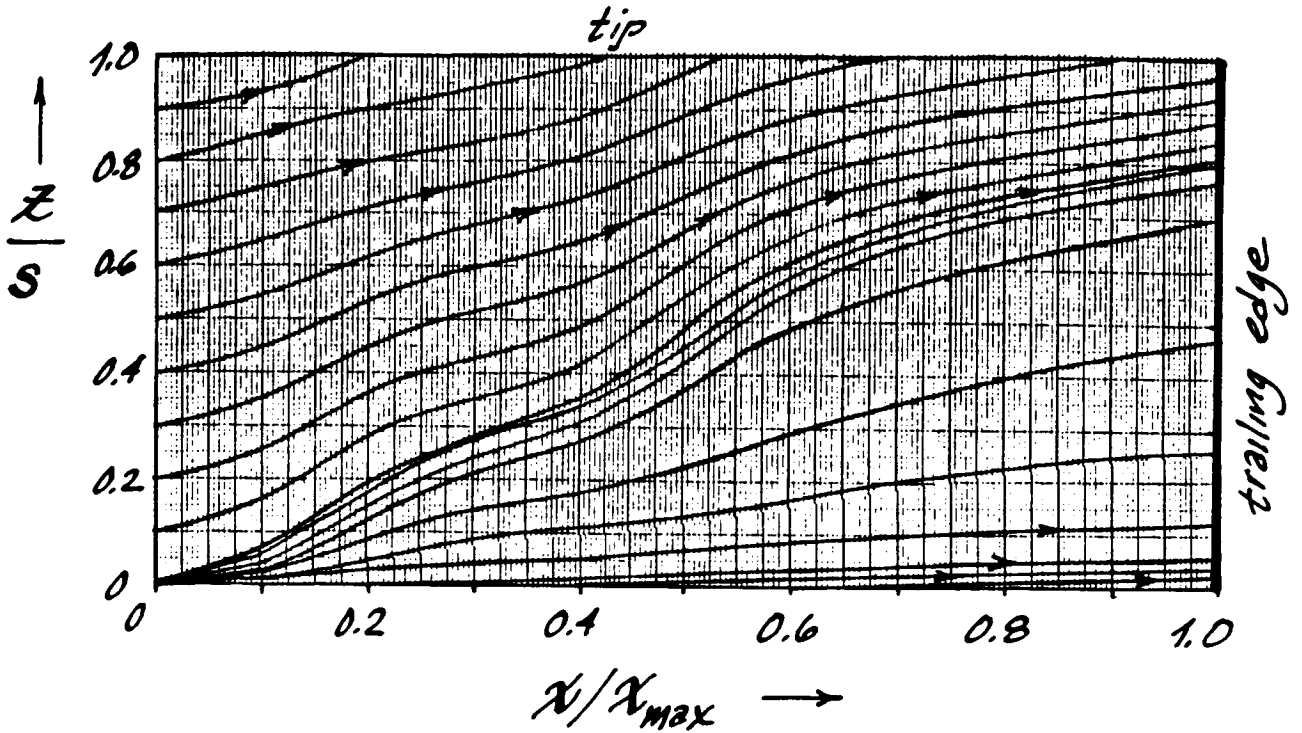


Fig. 3: Predicted streamline pattern in molten salt condensate layer along suction surface of test turbine rotor blade ( $\Omega = 6786 \text{ rad/s}$ ).

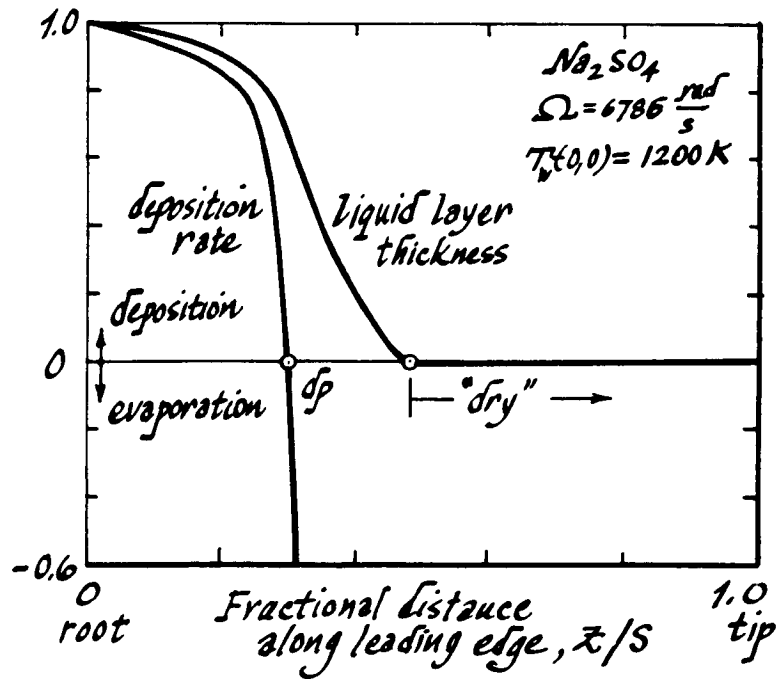


Fig. 4: Predicted molten salt layer thickness distribution along leading edge of root-cooled test turbine blade. (Note flow of liquid layer onto region of blade above prevailing dew point.)

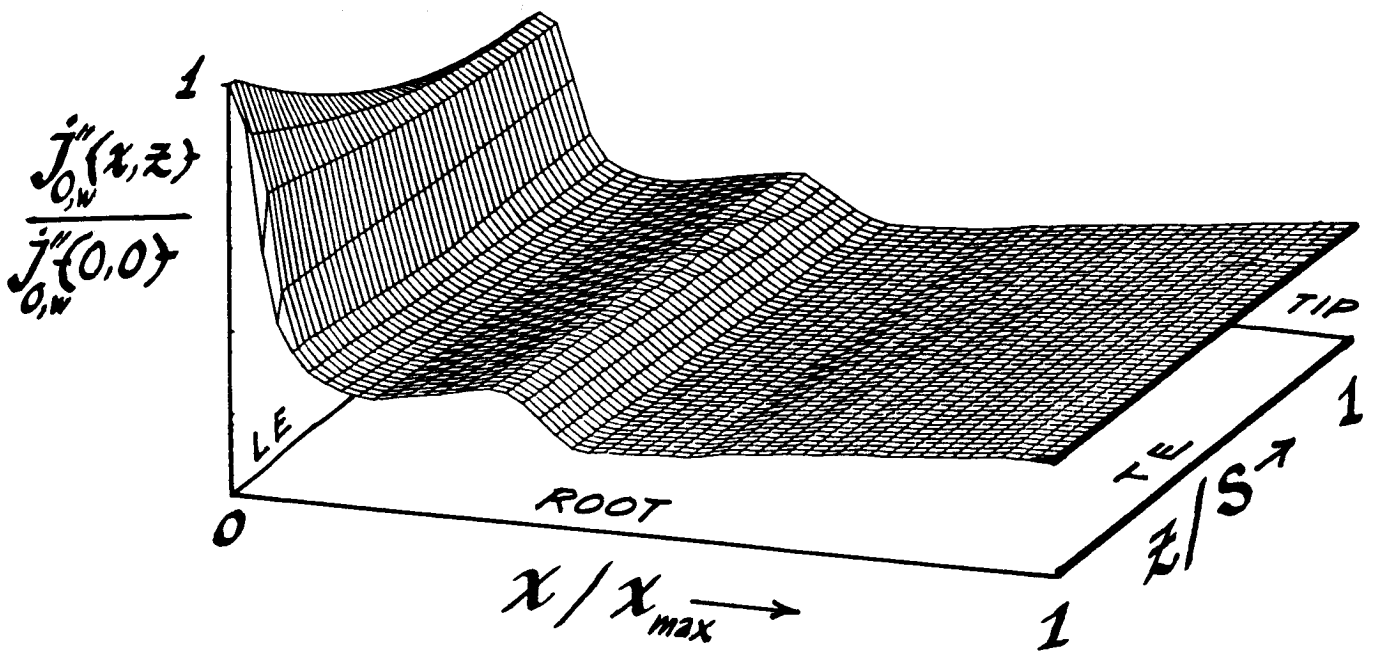


Fig. 5: Predicted distribution of metal oxide dissolution rates caused by molten salt condensate layer flow on root-cooled turbine rotor blade.

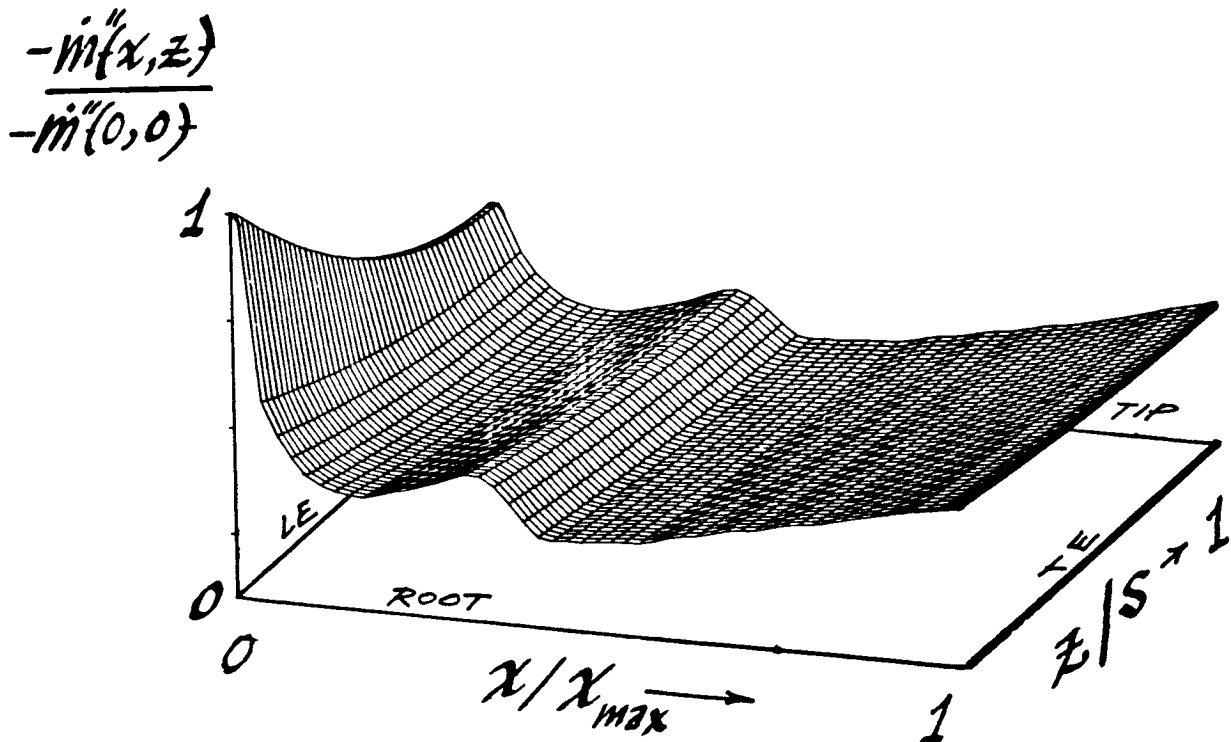


Fig. 6: Normalized  $\text{Na}_2\text{SO}_4$  arrival rate distribution (from vapor phase boundary layer) on turbine rotor blade suction surface.



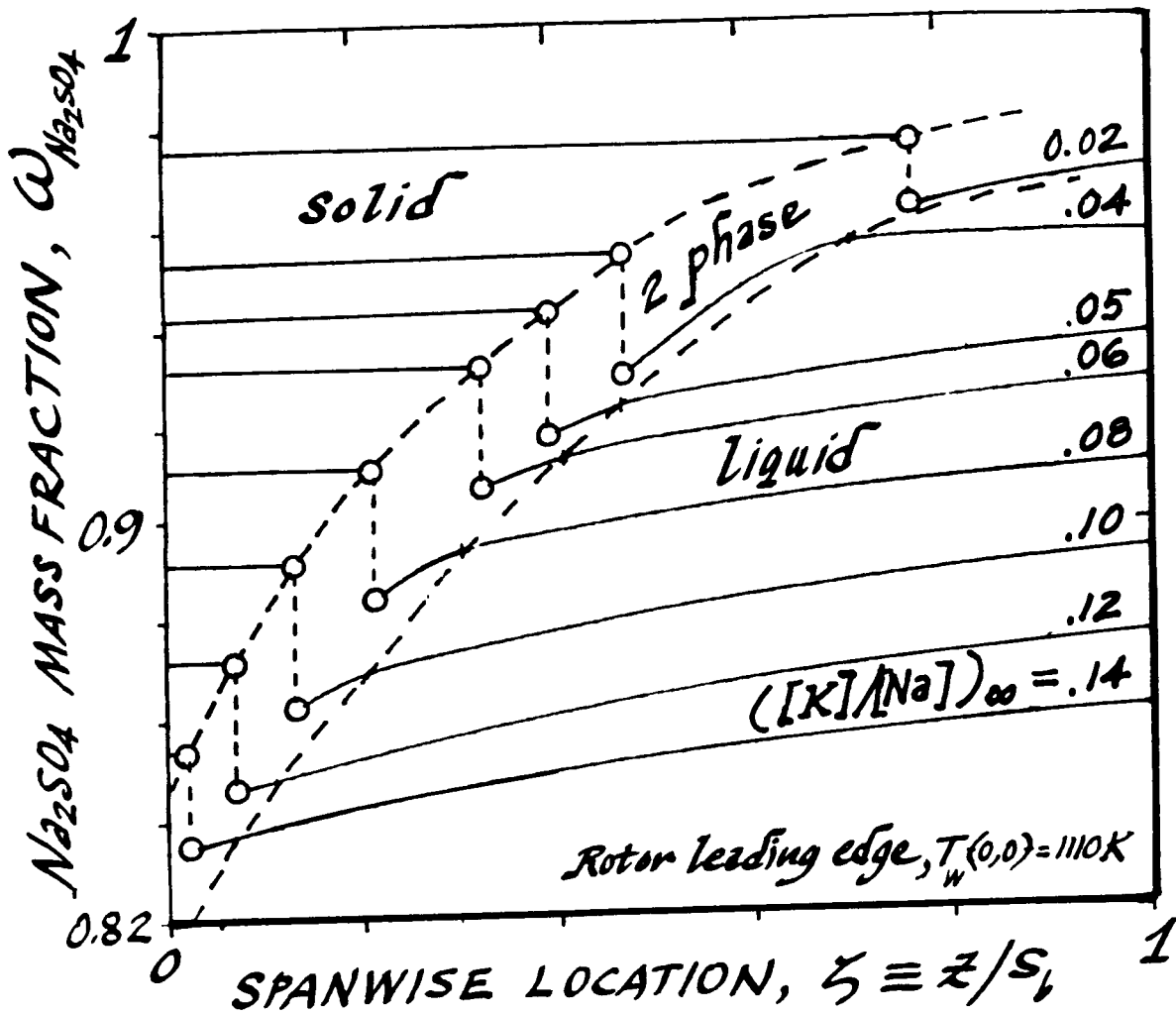


Fig. 7: Predicted distribution of condensate phase and composition along leading edge of a root-cooled turbine rotor blade ( $T_w(0,0) = 1110\text{K}$ ) vs. mainstream potassium: sodium ratio.